Supplementary material

Reengineering waste PET bottles into construction $BiOBr/Bi_4O_5Br_2$ heterojunction materials for highly selective photocatalytic oxidation of benzyl alcohol

Xuehai Ren [a], Yubin Wang [a, *], Jiang Li [b], Kefu Wang [b], Yanan Niu [b], Jide Wang [a, *] and Changyan Guo [a, *]

Key Laboratory of Oil and Gas Fine Chemicals, Ministry of Education, School of chemical engineering and technology, Xinjiang University, Urumqi, Xinjiang 830017, P. R. China

* Correspondence to: gcyslw@xju.edu.cn (Changyan Guo); awangjd@sina.cn (Jide Wang); wybin@xju.edu.cn (Yubin Wang)

Commercial BDC synthesis Bi-BDC process

Bi-BDC was prepared by one-pot hydrothermal method. In a typical experiment, 1.25 g BDC and 2.43 g $Bi(NO_3)_3 \cdot 5H_2O$ were added to 50 mL N, N-dimethylformamide (DMF) and stirred for 30 min until completely dissolved. The resulting suspension is then transferred to a 100 mL Teflon-lined stainless steel autoclave. Then the autoclave was sealed, heated at 150℃ for 12 h, cooled to room temperature, centrifuged to collect solid samples, and washed with DMF and methanol for 3 times, respectively. The solid samples were dried in a vacuum oven at 60℃ for 12 h to obtain Bi-BDC.[1,2]

Table S1. Commercial Bi-MOF economic accounting

Name	Unit price	dosage	Total price ($)	Total ($)	Yield (%)
$Bi(NO_3)_3 \cdot 5H_2O$	0.72 $/g	2.43 g	1.75		
BDC	0.21 $/g	1.25 g	0.26		
DMF	5.79 $/L	95 mL	0.55	4.86	41.03
MeOH	2.76 $/L	60 mL	0.17		
Electric charge	0.058 $/kWh	37.05 kWh	2.15		

Table S2. Economic accounting of waste PET synthesis Bi-MOF

Name	Unit price	dosage	Total price ($)	Total ($)	Yield (%)
$Bi(NO_3)_3 \cdot 5H_2O$	0.7 $/g	2.43 g	1.75		
Waste PET	0.28 $/kg	1.44 g	0.0004		
DMF	5.79 $/L	70 mL	0.41	4.54	42.12
MeOH	2.76 $/L	85 mL	0.23		
Electric charge	0.058 $/kWh	37.17 kWh	2.15		

Oven power: 1.55 kW; Vacuum drying chamber power: 1.45 kW; Centrifuge power: 0.45 kW; Local electricity price: 0.058 $/kWh; Local waste PET price: 248.28-317.24 $/ton, choose 275.86 $/ton calculation.

(1) The price of commercial synthetic Bi-BDC: 3.22 $/g.

(2) The price of PET synthesis Bi-BDC: 2.79 $/g.

A scale-up experiment (50 L high pressure reactor) was designed. The price of commercial BDC synthetic Bi-BDC: 3.22 $/g * 500 = 1610 $; The price of PET synthesis Bi-BDC: 2.79 $/g * 500 = 1395 $. Using the experimental method 500 times, the waste PET synthetic Bi-BDC is 215 $ cheaper than the commercial Bi-BDC.

Synthesis of BiOBr

BiOBr was synthesized by simple hydrothermal method. First, 2 mmol $Bi(NO_3)_3 \cdot 5H_2O$ was added to 50 mL of deionized water and stirred until dissolved. Then, 2 mmol NH_4Br was added and stirred for 30 min, and the solution was transferred to 100 mL of polytetrafluoroethylene lined stainless steel autoclave and at 140℃ for 12h. After cooling to room temperature, washing with water and anhydrous ethanol for 3 times, and vacuum drying at 60℃ for 12h, white BiOBr was obtained.[3]

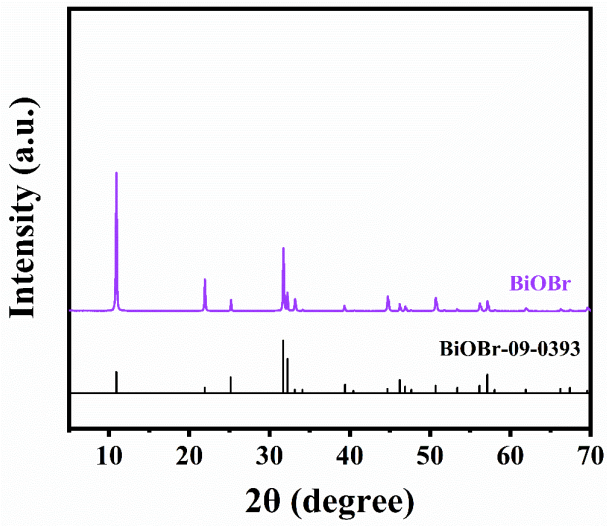

Figure S1. XRD patterns of BiOBr sample.

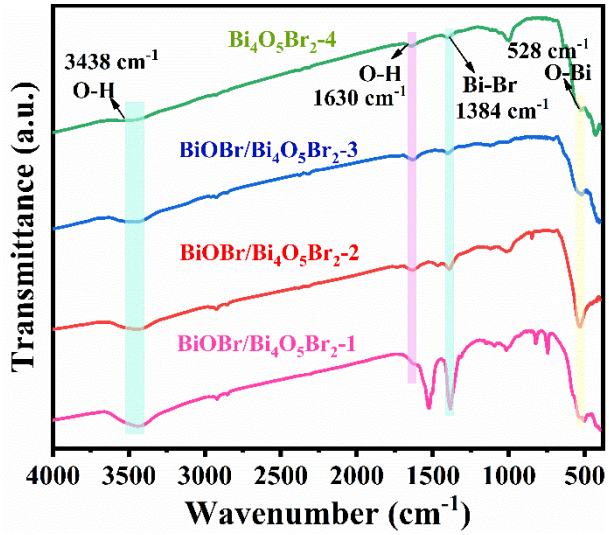

Figure S2. FT-IR spectra of $BiOBr/Bi_4O_5Br_2$-1, $BiOBr/Bi_4O_5Br_2$-2, $BiOBr/Bi_4O_5Br_2$-3 and $Bi_4O_5Br_2$-4.

Material characterization

The morphology of the catalyst was studied by field emission high-power scanning electron microscope (SEM) of SU8010 made by Hitachi. The phase structure of the

catalyst was analyzed by D8 Advance X-ray diffractometer (XRD) manufactured by Bruker, Germany. The test target was copper target, the scanning range was 5-90°, and the scanning speed was 10°/min. X-ray photoelectron spectroscopy (XPS) measurement uses monochromatic Mg Kα rays to emit x-rays (hv = 1,253.6 eV). Transmission electron microscopy (TEM) and high-resolution TEM (HRTEM) images were obtained using a FEI-Tecnai F20 microscope (200 kV), respectively. Photoluminescence (PL) spectra were determined by a Hitachi F-4600 fluorescence spectrometer. Electron spin resonance (ESR) tests are performed on a JES-FA200 spectrometer. Through the UV-4802S Ultraviolet–visible spectrometer (UV-vis) to study the visible light absorption of the catalyst, the test range is 200 - 1100 nm, with pure solid $BaSO_4$ crystal measured curve as the baseline, The measured reflectance profiles were then converted into UV-visible diffuse reflectance absorption profiles by Kubellka-Munk formula. The specific surface area was calcu-lated using the Brunauer-Emmett-Teller (BET) method. The mesopore size and distribution were calculated by the Barrett-Joyner-Halenda (BJH) method from desorption curves. The infrared spectra of the samples were obtained in the range of 400 - 4000 cm^{-1} using transmission mode on a Fourier-transform infrared spectrometer (FT-IR, Bruker EQUINOX - 55) to characterize the elements and functional groups.

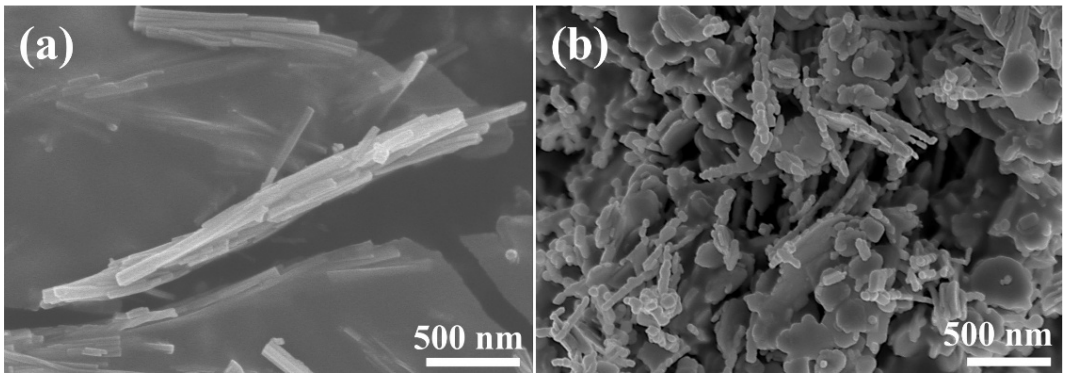

Figure S3. SEM images of (a) Bi-BDC and (b) BiOBr/$Bi_4O_5Br_2$-1.

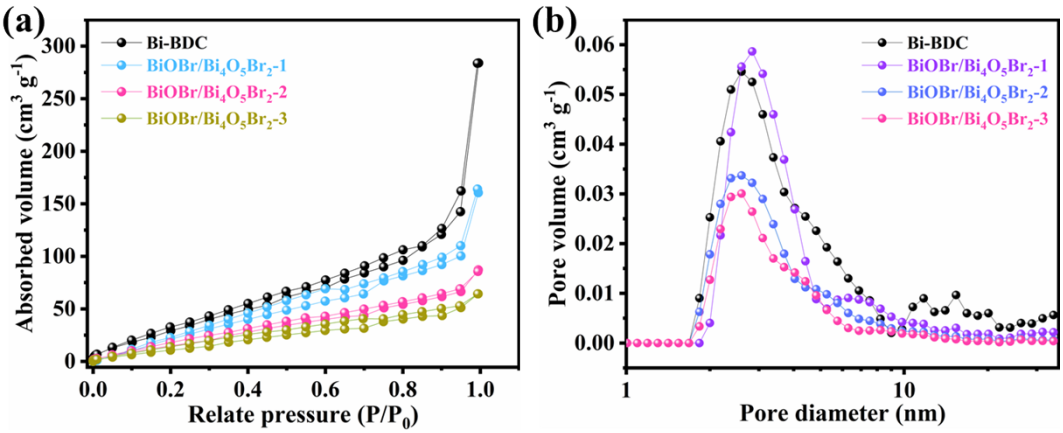

Figure S4. N_2 adsorption-desorption isotherms of Bi-BDC, BiOBr/$Bi_4O_5Br_2$-1 BiOBr/$Bi_4O_5Br_2$-2 and BiOBr/$Bi_4O_5Br_2$-3 and corresponding pore size distribution curves.

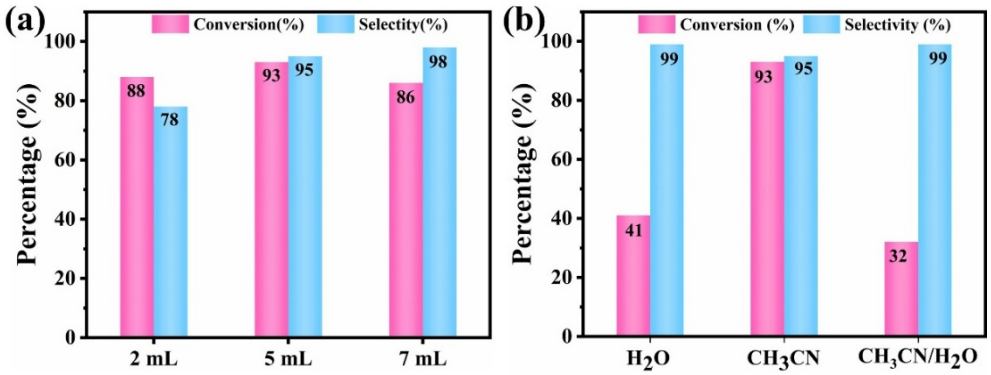

Figure S5. (a) effect of solvent amount on benzyl alcohol oxidation; (b) Effects of different solvents on benzyl alcohol oxygen (H_2O: 5 mL, CH_3CN:5 mL, CH_3CN/H_2O: 2.5/2.5 mL).

Table S3 Comparison of catalytic performance of Bi-based photocatalysts for selective oxidation of BA to BAD.

Photocatalysts	Conversion (%)	Selectivity (%)	Concentration (mmol)	Catalyst dosage (mg)	Light source	Time (h)	Extra oxidant Agent (O_2)	Ref.
1.0%Au/3D-BiOCl	48	>99	2.5	50	Vis. light	8		[4]
$Bi_4Ti_3O_{12}$	36	>99	0.1	10	Vis. light	5	+	[5]
BiOBr-sMS	51	100	0.5	20	Vis. light	2	+	[6]
0.8Br-BiOBr/Bi_2WO_6	40	>99	0.2	20	Vis. light	4	+	[7]
Au@Ag/BiOCl–OV	92	>99	0.1	50	Vis. light	10	+	[8]
3D-BiOCl@PDA	85	>99	0.5	50	Vis. light	2	+	[9]
BiOBr/g-C_3N_4	64	65	0.2	50	Vis. light	3	+	[10]
BiOI-CD-CdS	90	98	0.1	20	Vis. light	8	+	[11]
BiOBr/$Bi_4O_5Br_2$-2	93	95	0.1	10	Blue LED	3	+	This work

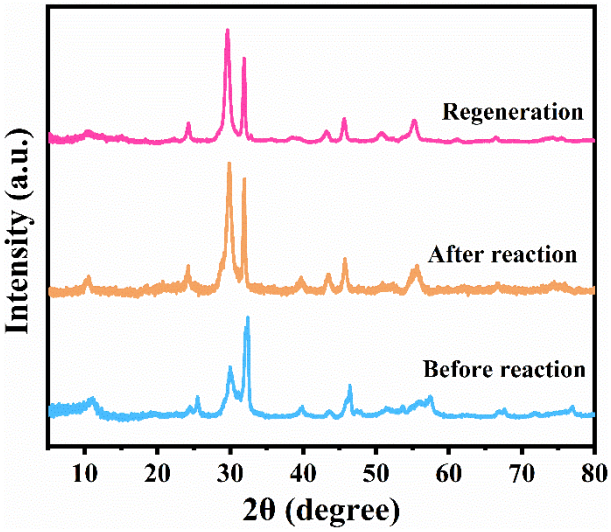

Figure S6. XRD patterns of BiOBr/$Bi_4O_5Br_2$-2 before and after cycling and after regeneration.

Table S4. Comparison of catalytic performance of different photocatalysts for BA selective oxidation to BAD.

Photocatalysts	Conversion (%)	Selectivity (%)	Cycle number	The conversion rate after the cycle (%)	Rate of decline (%)	Ref.
TiO_2	81	99	5	51	30.2	[12]
SnS/g-C_3N_4	73	>99	4	73	0	[13]
Co_1/TiO_2	99	98	5	>90	9	[14]
40-$CuBi_2O_4/WO_3$	55	99	5	47	7.8	[15]
$ZnIn_2S_4$14	57	96	4	20	37	[16]
40% $Ni(OH)_2$ on CdS-MoS_2	94	99	5	89	5.5	[17]
N-CQDs/CdS	60	99	5	52	8.12	[18]
7.5% CS QDs/T_3/TC QDs	98	99	5	98	0	[19]
BiOBr/$Bi_4O_5Br_2$-2	93	95	5	75	18	This work

Notes and references

1 L. Cao, J. Huang, X. Wu, B. Ma, Q. Xu, Y. Zhong, Y. Wu, M. Sun and L. Yu, *Nanoscale*, 2023, **15**, 19522–19532.

2 Y. Gao, F. Wang, J. Tang, C.-C. Wang, X.-H. Yi, Y. Wei, G. Liu, P. Wang, H. Fu, C. Zhao, X. Qiu and S. Yi, *Chem. Eng. J.*, 2024, **495**, 153651.

3 L. Jian, S. Li, H. Sun, Q. He, J. Chen, Y. Zhao and Y. Li, *Colloid Surfaces A*, 2022, **652**, 129919.

4 D. Yao, K. Liang, G. Chen, Y. Qu, J. Liu, R. Chilivery, S. Li, M. Ji, Z. Li, Z. Zhong and Y. Song, *J. Catal.*, 2023, **422**, 56–68.

5 M. Shen, Y. Shi, Z. Wang, T. Wu, L. Hu and L. Wu, *J. Colloid Interface Sci.*, 2022, **608**, 2529–2538.

6 Z. Wang, C. Liu, F. Chen and R. Chen, *Catalysts*, 2023, **13**, 958.

7 F. Wang, Y. Gu, Z. Yang, Y. Xie, J. Zhang, X. Shang, H. Zhao, Z. Zhang and X. Wang, *Appl. Catal. A: Gen.*, 2018, **567**, 65–72.

8 H. An, C. Deng, Y. Sun, Z. Lv, L. Cao, S. Xiao, L. Zhao and Z. Yin, *CrystEngComm*, 2020, **22**, 6603–6611.

9 R. Chilivery, R. Zhang, G. Chen, D. Yao, D. Fan, F. Lu and Y. Song, *Colloid Surface A*, 2023, **656**, 130415.

10 W. Wang, X. Cong, X. Zhang, W. Xu, J. Diao, Y. Bao and F. Guo, *J. Environ. Chem. Eng.*, 2025, **13**, 115552.

11 N. Verma and R. Ananthakrishnan, *ChemPhotoChem*, 2021, **5**, 545–558.

12 T. Hu, S. Zhu, Y. Yu, Z. Yue, Y. Wang, Y. Chang, W. Chen, L. Pei and J. Jia, *Mol. Catal.*, 2025, **575**, 114912.

13 Y. Li, C. Pan, G. Wang, Y. Leng, P. Jiang, Y. Dong and Y. Zhu, *New J. Chem.*, 2021, **45**, 6611–6617.

14 T. Wang, W. Li, Z. Wang, N. Lu, T. Wang, K. Wang, S.-B. Ren, W. Chen and G. Huang, *J. Alloys Compd.*, 2025, **1018**, 179233.

15 Z. Zhang, S. Hao, X. Duan, T. Wang, H. Li, G. Fan, Y. Zhao and J. Li, *J. Alloys Compd.*, 2023, **968**, 172209.

16 S. Ding, T. T. H. Duong, I. Medic, H. Lund, S. Bartling, N. Rockstroh, N. Steinfeldt and J. Strunk, *J. Environ. Chem. Eng.*, 2024, **12**, 113845.

17 C. Cui, X. Zhao, X. Su, W. Gao, J. Zhan, X. Zhang, G. Li, X. L. Zhang, Y. Sang and H. Liu, *J. Environ. Chem. Eng.*, 2021, **9**, 106416.

18 C. Liang, C. Wang, K. Xu, H. He, Q. Li, C. Yang and X. Gao, *Colloid Surface A*, 2022, **641**, 128559.

19 Y. Liang, P. Chen, Q. Li, C. Hu, S. Yang, K. Wu, J. Wu, G. Meng, J. Liu, Y. Tai and Z. Liu, *ACS Appl. Nano Mater.*, 2023, **6**, 6161–6171.